

T.1: Recent advances in materials joining at RRCAT

P. Ganesh^{1*}, A. P. Singh², A. Bhardwaj², Saranjeet Singh²,
Abhay Kumar² and Rakesh Kaul¹

¹Laser Materials Processing Division

²Design & Manufacturing Technology Division

*Email: ganesh@rrcat.gov.in

Abstract:

Materials joining is an ever emerging field to cater the specific needs of growing industry. Well established joining processes like fusion welding, diffusion bonding, tungsten inert gas brazing, etc. are continuously evolving with certain modifications in the form of fixturing and process modifications to tailor the weld metal properties compatible to various applications including low-magnetic-permeability, use in ultra-high vacuum applications, dissimilar joints, etc. The ease of implementation of new techniques at the shop floor and the economic aspect play an important role in acceptance of the new methodologies in the industry. The techniques developed at RRCAT Include new joint design, use of passive fixtures, minor modifications to existing welding and joining practices followed in the shop floor and have strong potential for deployment in industry. Present article summarizes the recent developments related to materials joining in the authors's lab, which essentially address the requirements of ongoing and future requirements related to particle accelerators at RRCAT.

1. Introduction

Construction of particle accelerators involve use of various types of materials for their specific properties. These materials must be joined to their conventional counterparts such as austenitic stainless steels to build the ultra-high vacuum (UHV) envelope. Joining of austenitic stainless steels also pose some very specific type of challenges from the perspective of particle accelerators. Other similar material joining challenges involve active metals like titanium, niobium, aluminium and their alloys due to the requirement of specified hygiene levels and environmental specification of cleanliness and humidity. These challenges must be met in order to build products that are compatible with general requirement of UHV and specific requirements coming from particle accelerator side.

Relative magnetic permeability (μ_r) is an important factor governing the choice of material for construction of vacuum chambers for particle accelerators; particularly those components that are either enclosed inside magnets or are placed in the vicinity of magnets. Austenitic stainless steel AISI 316L SS is a strong candidate for construction material of such vacuum chambers due to low values of μ_r (<1.05), ease of fabrication, ease of availability and competitive pricing. It is also a candidate for construction of helium vessels of superconducting radiofrequency (SRF) cavities for high-energy, high-power particle accelerators due to the possibility

of meeting the requirements of ASME B&PV Code Section VIII Division-1 for operation at 2 K temperature [1]. There are challenges in joining of austenitic stainless steels as welding must produce ferromagnetic delta-ferrite phase to avoid deleterious phenomenon of hot cracking and micro-fissuring. The ferromagnetic phase can attract the magnetic lines of forces while in operation and distort the charged particle's trajectory. This article presents the results of an experimental study, which attempted to limit the μ_r of weld metal to that of the base metal by introducing nitrogen-argon binary shield gas during gas tungsten arc welding (GTAW) of AISI 316L SS using bare ER 316L stainless steel filler metal [2]. An indigenous binary gas mixing system has been developed at RRCAT for reliable and economical deployment of the technology at particle accelerator laboratories.

Nitrogen-argon mixed shield gas requires two adaptations in the existing GTAW process usually deployed for GTAW of AISI 316L SS as nitrogen is a noble gas but not inert. The first one is to use gases of 5N purity and second one is to use gas lens system in the welding torch to avoid intermixing of environmental air with the shield gas flow. Gas lens system efficiently prevents the ingress of air into the stream of shield gas, which is due to Kelvin-Helmholtz instability at the interface of static air envelope and the shield gas. The instability is more pronounced in the turbulent flow regime as eddies formed at the interface lead to quick intermixing. The turbulence in shield gas due to Kelvin-Helmholtz instability can be delayed if the shield gas flow is maintained in laminar flow regime for longer distances [3]. The addition of gas lens improves the weld quality and reduces the gas consumption [4]. This article presents the results of studies carried out at author's laboratory involving use of gas lens and 5N purity shield gas.

Groundwork to build a mega-science project "Laser Interferometer Gravitational-Wave Observatory" – India (LIGO-India) is under progress as a part of the international network of gravitational wave observatories [5]. LIGO-India needs an 8 km long, ultra-high vacuum (UHV) compatible AISI 304L SS beam pipe. Each pipe is of 20 m length, 1239 mm outer diameter (OD), 3.2 mm thickness and straightness of 160 $\mu\text{m}/\text{m}$ length. These non-standard precision pipes need to be manufactured specifically using an automated continuous spiral welding pipe mill. Single pass and full penetration Activated-TIG (A-TIG) welding appears to be more suitable in this case due to its ease of deployment, minimal edge preparation and low distortion [6-9]. The study reported here essentially focuses on evaluation of the A-TIG welds of AISI 304L SS for UHV compatibility, which is not explored in earlier reports of A-TIG welding. The activating flux containing a mixture of five metal oxides was obtained from IGCAR, Kalpakkam [6].

Aluminium alloys of 5000 and 6000 series are popular materials for vacuum chambers of particle accelerators due to their paramagnetic nature and excellent UHV compatibility.

The Indus-2 (RRCAT) synchrotron radiation source's vacuum chambers are entirely made of aluminium alloys [10,11]. However, majority of gauges, pumps and piping connected to vacuum chambers are made of stainless-steel (SS). This necessitates deployment of aluminium alloys to SS bimetallic transition joints. Other than vacuum chambers, aluminium alloys-to-SS transition joints are also required for stray electron absorbers for industrial linear accelerators, cryogenic heat exchangers and components of irradiation capsules in nuclear reactors [12,13]. Such joints also find a lot of application in other industries as well [14]. The Al-SS joints are required for a variety of in-house applications like vacuum chambers, beam scraper assembly, cryogenic heat exchangers, cryo-module of superconducting radio frequency (SCRF) cavity, aluminium irradiation capsules, neutron sensitive ion chambers and ion chambers for environmental monitoring. Formation of brittle inter-metallic (IMC) phases at the weld interface during fusion welding of aluminium alloys and SS prohibits application of such processes [14-20]. Many of the friction welded aluminium alloy-to-SS transition joints of Indus-2 have failed after multiple baking cycles. In view of this, there is a need to develop an alternate way of joining aluminium alloys and SS. A study has been initiated at RRCAT to develop Al-SS joints through diffusion bonding, vacuum brazing and TIG brazing. The article presents some of the interesting results of these investigations.

Tantalum being a heavy metal ($Z=73$), is extensively deployed as an x-ray target material in electron beam based radiation processing facilities because of its refractoriness (T_m : $\sim 3000^\circ\text{C}$), excellent corrosion resistance, ductility and electrical and thermal conductivities. X-ray target assembly of Agricultural Radiation Processing Facility (ARPF) [21], requires dissimilar metal joining of 1.4 mm thick tantalum (Ta) sheet with an AISI 304L SS flange. Large difference in coefficient of thermal expansion (CTE) of materials being joined poses a problem in conventional vacuum brazing of 1.2 m long x-ray target component. Braze joining by using a TIG torch using a suitable filler without melting the parent materials is termed as TIG-brazing. TIG-Brazing due to localized heating and inherent control of heat input can be used as an alternate joining technique for a wide range of applications where normal braze joining or vacuum brazing methods fail due to large difference in CTE of materials being joined. An in-house study was undertaken with an objective of fabrication of x-ray target assembly of ARPF. The article presents the details of this study and successful demonstration of fabrication of first build (Ta-SS TIG braze joint) of the sub-size structure of x-ray target [22]. Exploring the use of titanium as a structural material for tantalum based x-ray target applications presents a promising solution. Open literature on joints of Ta with Grade-2 titanium reports tensile strength of 353 MPa. The metallurgical compatibility of both metals Ta and Ti with mutual solid solubility of *bcc* Ta in both forms of Ti (*hcp alpha* phase up to 882°C as well as high temperature *bcc beta* phase) enables formation of a sound joint. Notably, CTE for titanium ($9.9 \mu\text{m/m.K}$) and tantalum ($6.5 \mu\text{m/m.K}$) exhibits tolerable disparity with respect to other combinations, resulting in reduced thermal stress in the resultant joints. Other methods of

joining such as laser welding [23] and diffusion bonding [24] of tantalum to titanium have been reported with a tensile strength of about 260 MPa. However, certain limitations like joint fit-up requirements in laser welding, joint configuration in diffusion bonding and overall economic viability restrict their use. GTAW has a clear advantage over existing joining methods. The article presents the results of preliminary investigations of Ta-Ti joining using GTAW.

SCRF cavities will form important part of the upcoming high energy, high current proton accelerators. The high beta 650 MHz SCRF cavity would be enclosed in a cylindrical vessel to hold liquid helium (LHe). Titanium (Ti) is being considered as the material of construction of helium vessel. The LHe inlet supply line and return helium gas pipe line of the helium vessel would be made of AISI 316L SS. This requires a bi-metallic tubular transition joint between Ti and AISI 316L SS, operating at LHe temperature. Vacuum brazing and explosive welding are potential processes for joining these two dissimilar metals, as fusion welding leads to extensive cracking [25]. Explosive welded joint suffers from excessive shear stresses at the bond interface during subsequent fusion welding and cool down to 2 K temperature. The article presents the results of experimental study carried out at author's laboratory for vacuum brazing of Ti-pipe/316LSS flange with BVAg-8 braze filler metal (BFM) [26]. These joints remain under compression by design and have features that prohibit excessive heating during subsequent welding at both the ends.

Diffusion bonding, in spite of its many unique capabilities, has not been widely used for the joining process in fabrication of components due to high set-up cost, complex shape and size of the required joints for industrial applications [27]. An experimental study has been carried out at RRCAT with the aim of joining pipes of SS and Ti using passive fixtures with suitable CTE to generate required compressive stress between mating surfaces at elevated temperature to obtain diffusion bonding between titanium and austenitic SS tubes, without the use of a press. The article presents the new design of tube-to-tube joint assembly and results of microscopic examination of joints [28]. The new simplified approach will be useful in fabricating diffusion bonded joints in the vacuum furnaces using appropriate fixtures.

2. Materials and methods

2.1 Development of low-magnetic-permeability GTA welds

GTA welds were produced using 12 mm and 6 mm thick 316L SS with double and single V-grooves, employing a binary gas mixture of argon and nitrogen as shielding gas. Introduction of 1.5% nitrogen in the argon shielding gas resulted in nitrogen concentrations of about 0.15–0.2 wt% in the welds, compared to 0.04 wt% in welds without nitrogen. The resulting weld metal (WM) exhibited magnetic permeability (μ_r) of 1.033–1.035 close to μ_r of base metal, typically 1.02 to 1.05 (see Fig. T.1.1). Ferrite number (FN) values decreased significantly from 4.53 in WM to about 0.22–0.59 with 1.5% nitrogen addition. These welds met strength, ductility, and

impact test requirements of the ASME Boiler & Pressure Vessel Code (BPVC) for operation at room temperature and liquid helium temperature of 4 K (see Fig. T.1.2) [1]. This technique holds promise for fabricating BPVC-compliant 316L SS vacuum chambers and pressure vessels for particle accelerators, including helium vessels for SCRF cavities. Typically, pre-mix gas cylinders are employed for GTA applications due to the advantages of specific gas mixtures, such as achieving low magnetic permeability as in the case mentioned above. However, pre-mix binary gas cylinders face challenges in maintaining the consistency of the desired proportion of gases over time. This inconsistency occurs because the gases tend to stratify due to their density differences and associated buoyancy effects. Therefore, the authors have designed and developed an affordable binary gas mixer (see Fig. T.1.3) calibrated with standard binary gas analyzers. This system ensures cost-effectiveness and yields consistent weld joints.

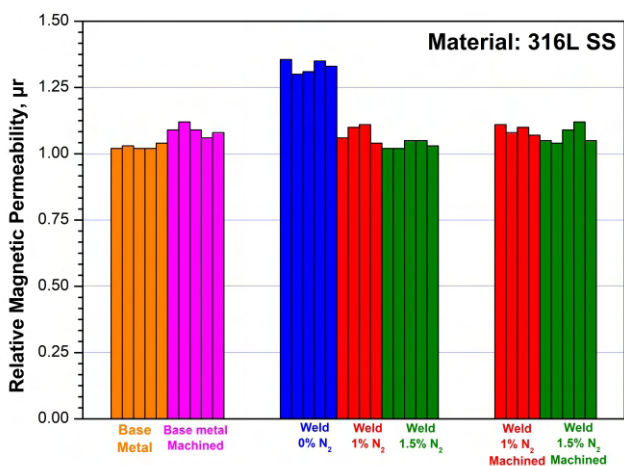


Fig. T.1.1: Relative magnetic permeability (μ_r) of base metal, machined base metal (left), weld metal with different nitrogen wt% (center) and weld metal after machining (right).

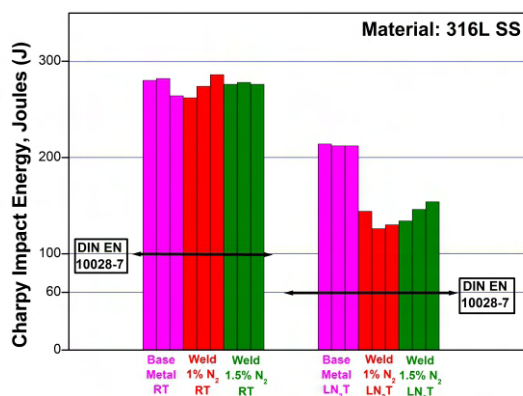


Fig. T.1.2: Charpy impact test results of base metal and weld metal at room temperature and liquid nitrogen temperature with different nitrogen (wt%) in shield gas. The black line represents the minimum required energy for failure at the respective temperatures. (DIN EN 10028-7:2008-02, pp17-21).

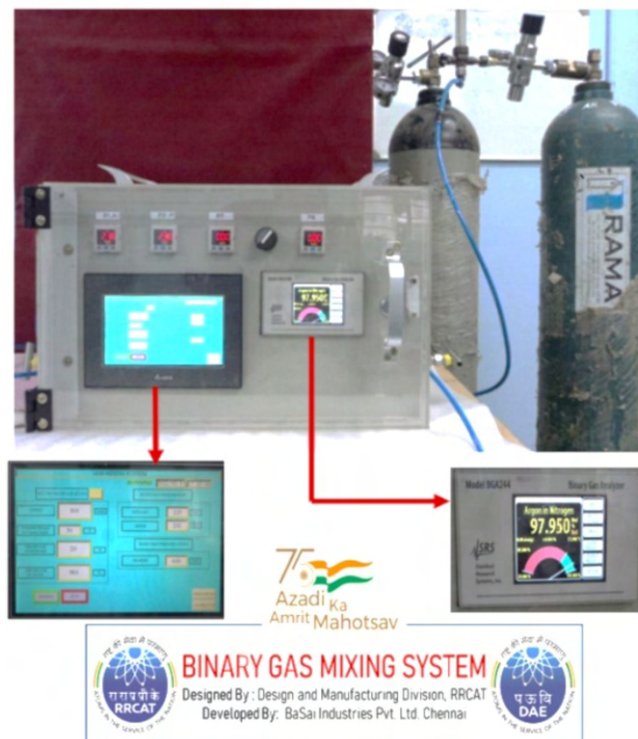


Fig. T.1.3: In-house developed binary gas mixer (Ar, N₂) calibrated with standard binary gas analyzer.

2.2 Deployment of gas lens for superior weld quality

TIG torch when incorporated with a gas lens generates a laminar flow of shielding gas. Figure T.1.4 depicts the gas flow image along the flow direction from torch orifice. It is evident that the laminar flow is limited only to 10-15 mm as compared to about 40-45 mm after incorporating gas lens. The waviness at the center of the image (Fig T.1.4(a)) is indicative of the turbulence whereas the straight edge in Fig. T.1.4(b) represents the laminar gas flow. As a result, a spatter-free, smooth weld bead without oxidation effects was achieved even with low shield gas flow rate (~6 lpm).

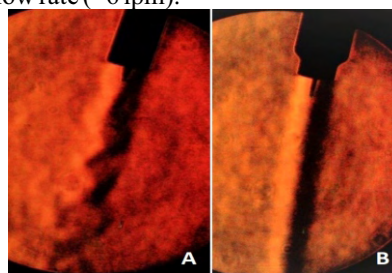


Fig. T.1.4: Gas flow of shielding gas as captured by Schlieren imaging technique: (a) turbulent flow without the gas lens & diffuser and (b) laminar gas flow with the gas lens & diffuser.

Additionally, an extra layer of gas diffuser was introduced (see Fig. T.1.5), enhancing performance while safeguarding the gas lens from potential damage as well. Gas diffusers, being cost-effective consumables, minimally impact welding expenses. These nozzles, typically made of ceramic or transparent quartz glass, can be reused multiple times and are replaced only if damaged by mishandling (see Fig. T.1.5). The integration of the gas lens system effectively addressed weld spatter issues, resulting in sound weld surfaces devoid of defects.

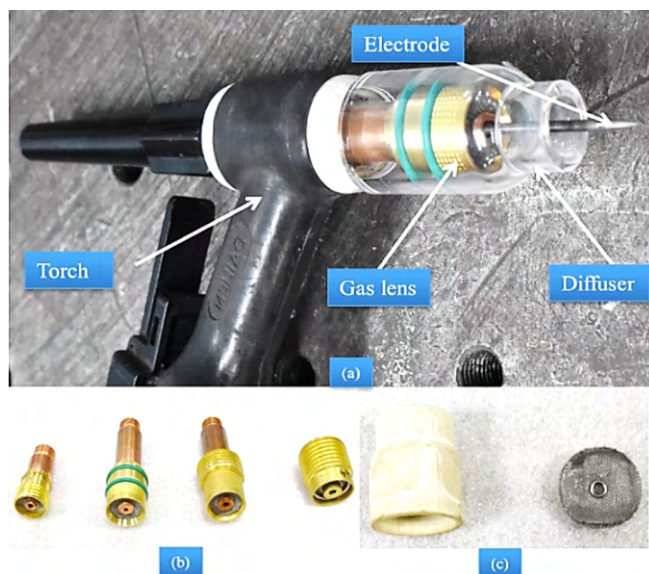


Fig. T.1.5: (a) Gas lens with diffuser mounted on welding torch, (b) various gas lens assemblies, and (c) diffuser.

2.3 Activated GTA welding for ultra-high vacuum applications

Investigations to explore autogenous activated GTA welding (A-TIG) for fabricating austenitic steel components for UHV applications has yielded promising results. Figure T.1.6 depicts the macro-structures of weld cross-section of normal TIG welded and A-TIG welded 3.2 mm thick sheet of 304L.

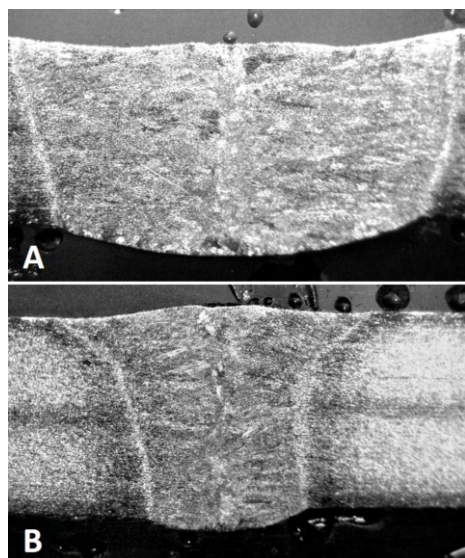
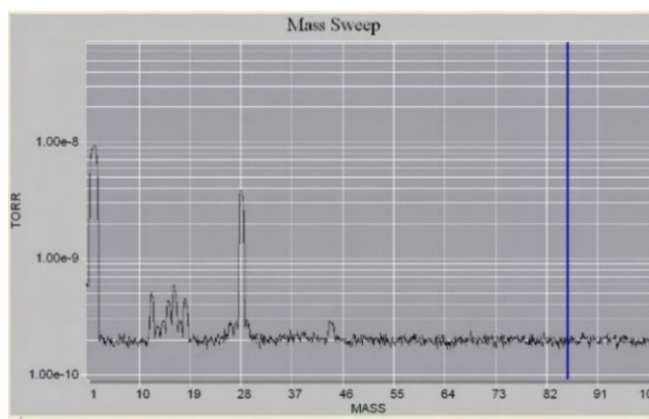
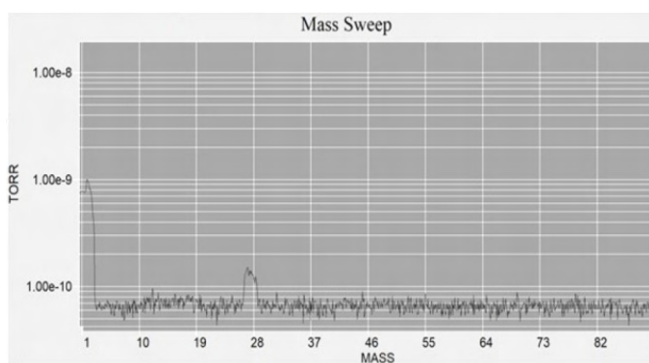


Fig. T.1.6: (a) Macro-structure of weld cross-section of normal GTA welded 3.2 mm thick sheet of 304L with slight concavity at the weld face and (b) macro-structure of weld cross-section of active GTA (A-TIG) welded 3.2 mm thick sheet of 304L with narrow fusion zone and heat affected zone without any concavity at weld face.

SEM analysis revealed that A-TIG welding did not introduce any deleterious inclusions due the use of activated flux. Residual gas analysis (RGA) findings provide conclusive evidence supporting the reliability of single-pass autogenous activated GTA welding for fabricating long tubular UHV compatible structures (see Fig. T.1.7) for LIGO application where stringent cleanliness and UHV are essential [8]. With respect to unbaked condition the RGA results show significant reduction of residual gases like H_2 , O_2 , N_2 and Ar after baking at 250 °C. A-TIG welding of 3.2 mm thick SS 304L sheets demonstrates that this process can be used for fabrication of austenitic steel components for UHV applications without any risk of encountering the deleterious constituents in the weld metal. Further, 316L SS sheets of higher thickness of up to 6 mm were welded using A-TIG process in 100% argon gas shield using bottom plate and gas lens in an autogenous mode in the butt configuration. This is in view of the fact that majority of the other in-house requirements fall in this thickness range. The resultant welds were completely free of any concavity and other defects in the fusion zone.



(a)



(b)

Fig. T.1.7: RGA plots during UHV qualification for (a) unbaked condition and (b) after 250 °C baking cycle. RGA tests confirm the leak tightness and a hydrocarbon free environment.

2.4 Development of aluminium to stainless-steel transition joints for ultra-high vacuum applications

Various methods of joining aluminum-to-stainless steel joints

are being investigated at DMTD, RRCAT. The aim is to develop robust joints suitable for diverse applications, including UHV and high temperature. Successful development of diffusion-bonded joints exhibiting vacuum compatibility has been achieved. Initially, diffusion bonding was conducted for fabrication of tensile test specimens using a specially designed fixture (see Fig. T.1.8), which generated the required compressive stress due to differential thermal expansion of materials involved. Joining was achieved at a temperature of 560 °C in a vacuum furnace with a heating duration of 10 minutes. The diffusion-bonded joints exhibited tensile strength of 50 Mpa.



Fig. T.1.8: Diffusion bonded tensile test samples along with the fixture used for joining.

Subsequently, tubular joints were fabricated (see Fig. T.1.9) with a specific design to accommodate differential thermal expansion. Additionally, threads are incorporated to enhance strength. Aluminum, which has higher coefficient of thermal expansion is placed inside compression ring of low CTE to prevent differential radial expansion and generate compressive stress on the threaded portion. To reduce longitudinal expansion, force is applied to the assembly using a high strength steel bolt of low CTE with respect to Al joining. The joints demonstrated no leaks under a helium background of 1×10^{-10} mbar.l/s.

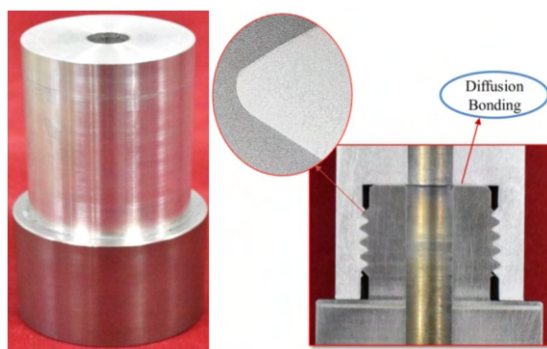


Fig. T.1.9: Tubular joint with a specific design to accommodate differential thermal expansion. Additionally, threads are incorporated to enhance strength.

2.5 Development of transition joints for x-ray target for Agricultural Radiation Processing Facility

2.5.1 Joining tantalum to stainless-steel through TIG brazing

X-ray targets used in the Agricultural Radiation Processing Facility (ARPF) are made of tantalum. However, for various other components, SS is utilized as the structural material. Consequently, tantalum-to-stainless-steel transition joints are necessary. Among the different braze fillers investigated for joining tantalum to SS; oxygen-free electronic (OFE) copper emerged as the most suitable filler. However, vacuum brazing of an actual component (1.2 m long) with OFE copper filler resulted in a vacuum leak of 1×10^{-5} mbar.l/sec due to thermal stresses developed during cool down. To mitigate the challenge posed by the difference in thermal expansion, an alternative joining method was explored, involving manual GTA weld braze in a controlled Ar atmosphere with the OFE copper filler. A sub-size model (110 mm x 55 mm x 12 mm) of the x-ray target assembly of ARPF was fabricated (see Fig. T.1.10). The joint sustained hydro testing of up to 6 bar and demonstrated vacuum leak tightness better than 1×10^{-10} mbar.l/s. Tensile strength of the joint made by GTA braze is about 90 MPa and the failure is ductile in nature.

Optical microscopy examinations reveal complete penetration of the braze filler into the joint, resulting in the formation of a sound joint without defects such as cracks and porosity (see Fig. T.1.11). Scanning electron microscopy (SEM) and energy dispersion spectroscopy (EDS) analysis indicate no melting of tantalum and SS or intermixing in the braze zone (see Fig. T.1.12). EDS analysis of the joint cross-section displayed the formation of a thin layer of $\sim 5 \mu\text{m}$ consisting of Ta-Fe/Cr/Cu intermetallic compounds in areas where there was excessive filler deposition and associated higher heat input. Therefore, controlled heat input, appropriate gas shielding, and filler compatibility with both parts to be joined are crucial for achieving sound joints through GTA brazing. Another method involving TIG-braze joining of Ta-SS using eutectic filler (BVAg-8) is attempted in open atmosphere. The use of BVAg-8 has an added advantage of good wetting with Ta and SS, lower melting temperature (780°C) and scope for better control of manual TIG brazing operation. The fabricated joints (sheet to sheet) were free from melting of Ta and SS and other defects like lack of filling or cracks and the tensile strength is 250 MPa. Further work is under progress to qualify these joints for end use requirements.

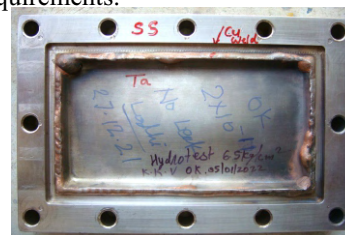


Fig. T.1.10: Tantalum brazed to 316L SS using GTA braze, employing OFE copper filler in a controlled argon atmosphere. The brazing involved a 1 mm thick tantalum sheet centrally positioned and joined along its rectangular perimeter.

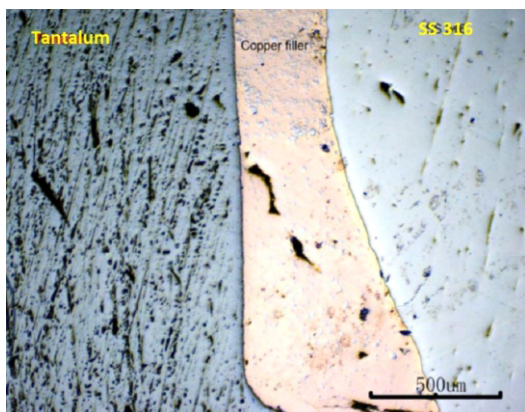
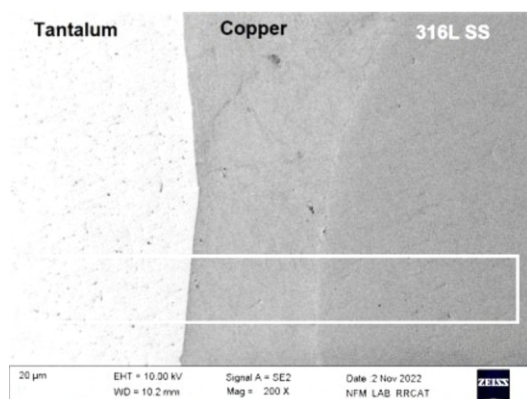
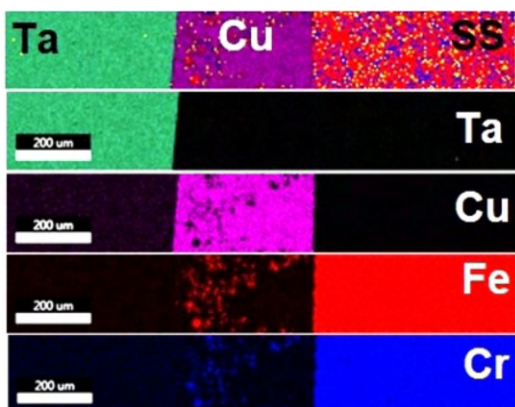


Fig. T.1.11: Optical micrograph of the cross-section of the tantalum-SS GTA brazed joint reveals complete penetration of the OFE copper filler into the joint gap, with no evidence of melting at the edges of the SS and tantalum.



(a)



(b)

Fig. T.1.12.: (a) SEM image of joint cross-section with distinct interfaces of tantalum-copper and copper-SS without any intermixing and (b) EDS elemental mapping depicting the distribution of various elements in zone marked in the SEM image.

2.5.2 Joining tantalum to titanium through TIG welding

Continuing from previous developments, the project now focuses on joining tantalum to titanium sheet material (1.6 mm thick) using autogenous GTA welding with pure titanium filler. Special welding equipment such as gas lens, gas diffuser, back purging box, and trailing shield are utilized without the need for a glove box. Effective positioning of the tungsten electrode minimizes tantalum melting, resolving liquation cracking issues stemming from the significant difference in melting points.

Optical macrograph of GTA welded sample (1.6 mm thick) (see Fig. T.1.13) of tantalum to titanium alloy revealed complete penetration without any porosity or other defects. Tantalum exhibited minimal/no melting due to its high melting point, while titanium sheet has completely melted, forming a clean interaction layer in the weld joint. Elemental mapping of the cross-section (see Fig. T.1.14) indicates no melting of tantalum. There is no evidence of any deleterious second phase/ intermetallic layer. The ultimate strength of the joints is found to be in the range of 352-406 MPa, which is more than the strength of tantalum. The tensile specimen also showed signs of necking and ductile fracture in the weld region. The welded flange to sheet joint has been inspected for hermeticity and high pressure test. The joint exhibited an impressive hermeticity with a leak rate of 9.7×10^{-11} mbar.l/sec. The welded job passed the hydrostatic pressure test at 6 bar, which is more than the operating working pressure of 4 bar.

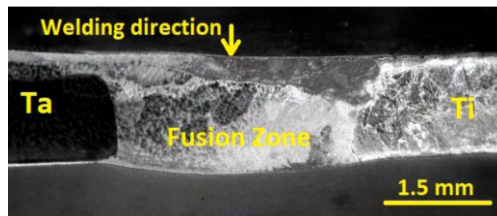


Fig. T.1.13: Cross-section of weld macro-structure of GTA weld of Ta and Ti with Ti filler.

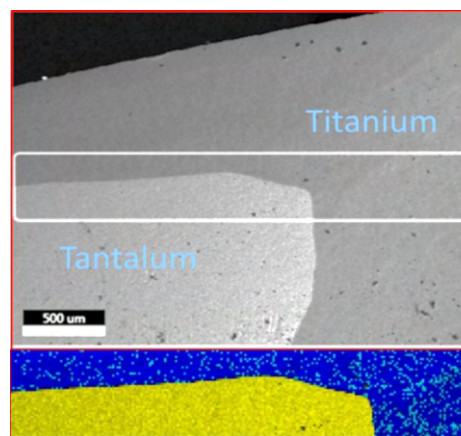


Fig. T.1.14: SEM image of joint cross-section along with the elemental distribution in the marked rectangular zone at Ta-weld interface of weld cross-section (yellow: Ta; blue: Ti).

2.6 Vacuum brazing of titanium and stainless steel

The present experimental study was carried out to address the in-house requirements related to SCRF cavity structural components. The challenge is joint design to accommodate the differential thermal expansion (Ti and SS) and braze gap control during brazing. Vacuum brazing was performed to join titanium pipe and 316L SS flange with BVAg-8 braze filler metal (BFM). Figure T.1.15 depicts the final joint of titanium tube to SS flange. Figure T.1.16 shows the microstructure of the joint cross-section with a thin layer of reaction bonded Cu-Ti intermetallic layer at the Ti- braze interface. Notable features of the process include (i) 5-10 μm nickel electroplating as a diffusion barrier on SS faying surface for preventing possible iron migration towards titanium and improving surface wettability for BFM and (ii) use of 304 SS plug, shrunk fit into Ti-pipe, for achieving dimensional and profile accuracy of Ti-pipe during machining and controlling joint gap during brazing process. The brazed joint displayed uniform joint thickness and acceptable level of hermeticity (helium leak rate less than 2×10^{-10} mbar.l/sec) and sustained six thermal cycles between 293 K and 77 K. Shear strength of Ti-SS brazed specimens, made in sandwich configuration, was found to be in the range of 50-60 MPa, with failure occurring at Ti/braze interface [22].

The results of the present study have demonstrated that vacuum brazing of titanium pipe to nickel-plated 316LSS flange with BVAg8 filler resulted in sound transition joint with satisfactory shear strength of about 50-60 MPa and uniform joint thickness of about 50 +/- 10 μm . Vacuum brazed component displayed helium leak tightness better than 5×10^{-10} mbar.l/s and also withstood six numbers of thermal cycles between 300 K and 77 K without any degradation in joint's hermeticity; thereby establishing its suitability to withstand service-induced low cycle fatigue conditions.

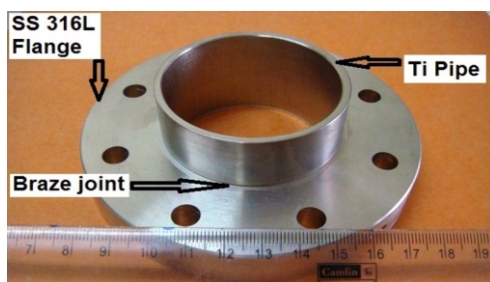


Fig. T.1.15: Braze joint of titanium tube to SS flange.

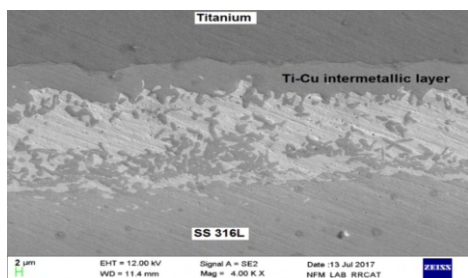
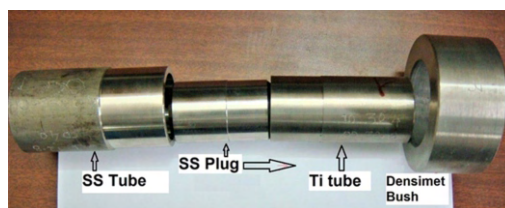


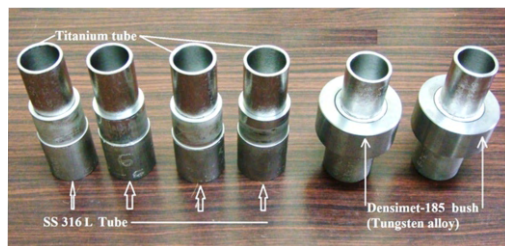
Fig. T.1.16: Microstructure of the braze cross-section with titanium-copper intermetallic layer at titanium braze interface.

2.7 Diffusion bonding of Ti & SS tubes

The study involved diffusion bonding between titanium and type 316L SS tubes in a lap configuration, utilizing fixtures such as a densimet sleeve on the outer diameter and a 304 SS plug on the inner diameter (see Fig. T.1.17). This setup generated the necessary compressive stress at the mating interface. Heating the assembly in a vacuum furnace at 900 °C for 120 minutes followed by furnace cooling resulted in diffusion bonded joints. Joints were prepared with titanium tubes of varying wall thicknesses (1.2-1.8 mm). All joints exhibited helium leak rates better than 2×10^{-10} mbar.l/sec and shear strength of 45-50 MPa. Microscopic examination revealed sound joints with an interdiffusion zone of 3-5 μm .



(a)



(b)

Fig. T.1.17: (a) Machined components set before assembly and (b) diffusion bonded titanium-SS tubular joints.

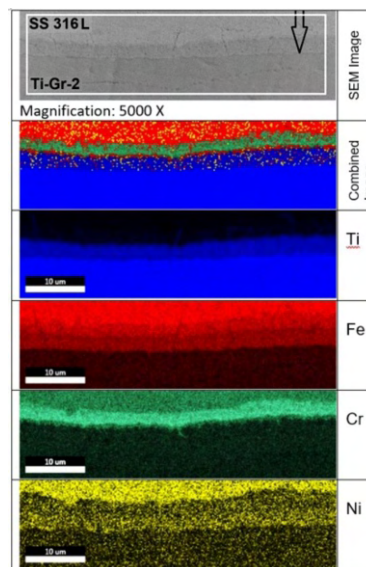


Fig. T.1.18: SEM image of the joint cross-section and the EDS mapping of elements in the region marked in the SEM image shown at top with segregation of titanium, chromium and iron at the joint interface.

Intermetallic compounds, specifically Ti-Fe/Cr, formed at the joint interface through reaction bonding at 900 °C are responsible for the joining (see Fig. T.1.18). Despite a shear strength of approximately 50 MPa, the SS-Ti tube-tube joint exhibits a high load-carrying ability of over 40 kN due to the compressive stress developed at the joint interface. Enhancements in joint strength can be achieved by controlling dimensional tolerances and reducing associated eccentricity. This study demonstrates successful diffusion bonding of titanium and austenitic stainless steel tubes using passive fixtures without the need for pressing [28]. This technique shows significant promise for joining dissimilar metallic materials, particularly tubes with wide differences in coefficient of thermal expansion, suitable for applications in the chemical and nuclear industries.

3. Conclusions

This article presents a brief summary of the recent developments in the domain of materials joining at RRCAT. The highlights include successful development/demonstration of:

- (i) Low-magnetic-permeability welds of 316L SS using nitrogen alloying (using an in-house made binary gas mixture) targeted for use in critical applications in particle accelerator structural components.
- (ii) Use of gas lens and diffuser with TIG torch for obtaining superior welds in the open atmosphere which otherwise necessitate controlled atmosphere for handling active metal welding.
- (iii) Active-TIG welding of AISI 304L for LIGO-India application and development of aluminium to stainless-steel transition joints for ultra-high vacuum applications.
- (iv) Joining tantalum to 316L stainless steel using TIG-brazing and Ta–Ti joining by TIG welding in open atmosphere using gas lens for targeted x-ray target application of an electron accelerator.
- (vi) Diffusion bonding of Al-SS and tube to tube diffusion bonding of Ti–SS using passive fixtures without the use of press.

The above developmental activities and the ongoing research will provide a strong knowledge base for the present and future joining requirements of RRCAT/DAE in particular and joining industry in general.

Acknowledgements

Authors sincerely acknowledge the contribution of all the colleagues of UHVTS and LMPD for conducting these studies. Special thanks are due to Shri Vineet Kumar Lal and staff members of vacuum brazing furnace for their unconditional support for carrying our various experiments. Authors gratefully acknowledge the colleagues from LFMD (Smt Rashmi Singh and Shri M. K. Singh) for their help in conducting the SEM and EDS analysis. Dr. P. Ram Sankar, Head, Chemical Treatment Lab and his team members have provided valuable contributions for electroplating related to these developmental studies. The valuable contribution of colleagues from LMPD, Shri Ram Nihal Ram,

Shri Abhijit Chowdhury, Shri Dinesh Nagpure and Shri Ram Kishor Gupta is gratefully acknowledged.

References:

- [1] ASME Boiler & Pressure Vessel Code, Section VIII Division-1, The American Society of Mechanical Engineers, 2019 Edition. New York: Table ULT-23, p265; UHA-51(a)(3).
- [2] A Kumar, P Ganesh, V. K. Sharma, M. Manekar, R. K. Gupta, R. Singh et al., “Development of Low-Magnetic-Permeability Welds of 316L Stainless Steel”, *Welding Journal*, Research supplement, Vol. 100, 323-s 337-s, (2021).
<https://doi.org/10.29391/2021.100.029>.
- [3] URL: <https://sea.itw welding.com/Article/11/Article-Using-a-Gas-Lens-for-TIG-Welding-Applications> (Visited on 12 March 2024).
- [4] URL: <https://weldingweb.com/vbb/threads/38318-Noob-Gas-Lens-Basics-for-TIG-Applications> (Visited on 12 March 2024).
- [5] <https://www.ligo-india.in/> (Visited on 12 March 2024).
- [6] Penetration enhancing Activated Flux for TIG welding of Stainless Steels – Bhabha Atomic Research Centre (BARC);
<https://www.barc.gov.in/technologies/ch44igcar/index.html>.
- [7] M. Vasudevan, “Effect of A-TIG welding process on the weld attributes of type 304LN and 316LN stainless steels”, *Journal of Materials Engineering and Performance* 26(3), 25-36 (2017).
- [8] Hemant Kumar, Singh N. K., “Performance of activated TIG welding in 304 austenitic stainless steel welds”, *Materials Today: Proceedings*, 4:9914–9918 (2017).
- [9] Ashutosh Pratap Singh et al., “Characterisation of A-TIG welding of AISI 304L for ultra-high vacuum application”, *National Welding Seminar (NWS) 2022*, 19-21 January 2023, Chennai, Tamilnadu, India: C-023
- [10] D. D. Bhawalkar, G. Singh and R. V. Nandedkar, “Synchrotron Radiation Sources Indus-1 and Indus-2”, *PRAMANA- J. Phys. Indian Acad. Sci.*, 50(6), p 467–484 (1998).
- [11] S. K. Sharma, Honey Gupta, Vikas Jain et al., "Investigation of Ultra-High Vacuum Compatible Weld Joints of AA5083 and AA6061 Materials for Synchrotron Radiation Source", *J. Mater. Eng. Perform.* Vol. 31, 4795–4810(2022).
<https://doi.org/10.1007/s11665-022-06589-8>.
- [12] D. Popov, K. Fikiin, B. Stankov, G. Alvarez, M. Youbi-idrissi, A. Damas, J. Evans, T. Brown, "Cryogenic heat exchangers for process cooling and renewable energy storage : A review", *Appl. Therm. Eng.* 153, 275–290 (2019).
<https://doi.org/10.1016/j.applthermaleng.2019.02.106>.
- [13] Szontagh, Endre, Eva, Andras, Koevari, Tiborne,

- "Application of aluminium in nuclear power plants; the role of corrosion under breakdown conditions within the hermetic zone", *Magy. Alum.* 24 153–159 (1987).
- [14] M. Zhao, X. Wang, S. Tang, Zhigang Lin, H. Chen, "Determination and characterization of heat input, microstructure and performance in cold metal transfer welding-brazing of dissimilar AA6061-T6 to SS304 sheets", *Trans. Indian Inst. Met.* (2023).
- [15] T. Murakami, K. Nakata, H. Tong, M. Ushio, "Dissimilar Metal Joining of Aluminum to Steel by MIG Arc Brazing Using Flux Cored Wire", *ISIJ Int.* 43 1596–1602 (2003).
- [16] J. L. Song, S. B. Lin, C. L. Yang, C. L. Fan, G. C. Ma, "Analysis of intermetallic layer in dissimilar TIG welding – brazing butt joint of aluminium alloy to stainless steel", *Sci. Technol. Weld. Join.* 15, 213–219 (2010).
<https://doi.org/10.1179/136217110X12665048207610>.
- [17] H. T. Zhang, J. C. Feng, P. He, H. Hackl, "Interfacial microstructure and mechanical properties of aluminium–zinc-coated steel joints made by a modified metal inert gas welding– brazing process", *Mater. Charact.* 58, 588–592 (2007).
<https://doi.org/10.1016/j.matchar.2006.07.008>.
- [18] C. Muralimohan, B. Srinivas, N. Abhishek, T. Ramachandraiah, S. Karna, D. Venkateswarlu, "Dissimilar Joining of Stainless Steel and 5083 Aluminum Alloy Sheets by Gas Tungsten Arc Welding-Brazing Process Dissimilar Joining of Stainless Steel and 5083 Aluminum Alloy Sheets by Gas Tungsten Arc Welding-Brazing Process", *Mater. Sci. Eng.* 330, 1–7 (2018).
<https://doi.org/10.1088/1757-899X/330/1/012048>.
- [19] H. He, S. Lin, C. Yang, "Weld Brazing a Joint of Aluminum to Stainless Steel", *Weld. J.* 365–378 (2019).
<https://doi.org/10.29391/2019.98.030>.
- [20] S. Babu, S. K. Panigrahi, G. D. J. Ram, P. V. Venkitakrishnan, R. S. Kumar, "Cold metal transfer welding of aluminum alloy AA 2219 to austenitic stainless steel", *J. Mater. Process. Tech.* 266 (2018).
<https://doi.org/10.1016/j.jmatprotec.2018.10.034>.
- [21] URL:
<https://www.rrcat.gov.in/newsletter/NL/nl2019/issue2/pdf/T1.pdf> (visited on 12 March 2024).
- [22] P. Ganesh, et al., "Joining tantalum and type 316L stainless steel using TIG-brazing for application in x-ray target assembly of agriculture radiation processing facility", *Proc. National Welding Seminar 2022*, 19–21 January 2023, Chennai, Tamilnadu, India. Article No.: C008.
- [23] D. Grevey, V. Vignal, Issam Bendaoud, P. Erazmus-Vignal, I. Tomashchuk, et al., "Microstructural and micro-electrochemical study of a tantalum-titanium weld interface", *Materials & Design* 87, 974–985 (2015).
[10.1016/j.matdes.2015.08.074](https://doi.org/10.1016/j.matdes.2015.08.074).
- [24] K. Nishio, H. Masumoto, H. Matsuda, H. Ikeda, "Diffusion bonding of tantalum to titanium", *Quart. J. Jpn. Weld. Soc.* 21 302–309 (2003).
- [25] A. Winiowski, "Mechanical and structural properties of joints of stainless steel and titanium brazed with silverfiller metals containing tin", *Archives of metallurgy and materials* 55(4), 2010,
[DOI: 10.2478/v10172-010-0001-9](https://doi.org/10.2478/v10172-010-0001-9).
- [26] P. Ganesh et al., "Vacuum brazing of titanium/316L stainless steel transition joint for application in helium vessel of superconducting RF cavities", *Proc. Indian Institute of Welding International Congress (IIW-IC)*, 7–9 Dec. 2017, Chennai, Tamilnadu India; Paper ID C066.
- [27] T. Vigraman, D. Ravindran and R. Narayanasamy, "Effect of phase transformation and intermetallic compounds on the microstructure and tensile strength properties of diffusion bonded joints between Ti-6Al-4V and AISI 304L", *Materials and Design* 36, 714–727 (2012).
- [28] P. Ganesh et al., "A new approach of diffusion bonding for joining titanium and austenitic stainless steel tubes", *National Welding Seminar (NWS) 2022*, 19–21 January 2023, Chennai, India. Article ID: C-007.